A Novel Dual-band Printed Diversity Antenna for Mobile Terminals

Published in:
IEEE Transactions on Antennas and Propagation

Document Version:
Early version, also known as pre-print

Queen's University Belfast - Research Portal:
Link to publication record in Queen's University Belfast Research Portal

A Novel Dual-band Printed Diversity Antenna for Mobile Terminals

Yuan Ding, Zhengwei Du, Ke Gong, and Zhenghe Feng

Abstract—**A novel dual-band printed diversity antenna is proposed and studied. The antenna, which consists of two back-to-back monopoles with symmetric configuration, is printed on a printed circuit board (PCB). The effects of some important parameters of the proposed antenna are deeply studied and the design methodology is given. A prototype of the proposed antenna operating at UMTS (1920 ~ 2170 MHz) and 2.4-GHz WLAN (2400 ~ 2484 MHz) bands is provided to demonstrate the usability of the methodology in dual-band diversity antenna for mobile terminals. In the above two bands, the isolations of the prototype are larger than 13 dB and 16 dB, respectively. The measured radiation patterns of the two monopoles in general cover complementary space regions. The diversity performance is also evaluated by calculating the envelope correlation coefficient, the mean effective gains (MEGs) of the antenna elements and the diversity gain. It is proved that the proposed antenna can provide spatial and pattern diversity to combat multi-path fading.**

Index Terms—**Diversity antenna, diversity gain, dual-band antenna, envelope correlation coefficient, mean effective gain (MEG).**

I. INTRODUCTION

Antenna diversity is a well-known technique to enhance the performance of wireless communication systems by reducing the multi-path fading and co-channel interference [1]. Nowadays, in a cellular communication system, it is easy to be implemented at the base station where antenna separations of many wavelengths are readily available. However, in order to improve the quality of wireless downlink signal, more than one antenna is necessary for the terminal side. In this kind of mobile terminal, two or more antenna elements are envisaged and the restricted space available for antenna is an open issue [2].

Most designs of diversity antenna in mobile terminals are for WLAN operation [3][4], and they are applied in the PCMCIA

card of a laptop. In [5], a dual-band printed diversity antenna for 2.4/5.2-GHz WLAN operations was proposed. The antenna consists of two orthogonal C-shaped monopoles with a symmetric configuration. A protruding T-shaped stub at the ground plane is used to increase the isolation between the two elements. In [6], based on the deep study on bandwidth enhancement and size reduction of the microstrip slot antenna, a diversity antenna of dual L-shaped slots with a bandwidth of 2.52 to 6.4 GHz was presented. The isolation between two ports across the whole bandwidth is controlled well. Unfortunately, it cannot cover the most usual bands, such as UMTS and 2.4-GHz WLAN, in the limited antenna volume. Another design of dual-helical antenna for diversity on mobile handsets was provided recently [7]. However, the relatively large antenna volume and the strong coupling between its two elements restrict its application. In [8], C. C. Chiau et al. introduced a four-element diversity-antenna for PDA terminals operating at 5.2 GHz. But it should be pointed out that the large metal case, $110 \times 75 \times 10$ mm^3, which represents the circuit board of a PDA, as well as the three-dimensional configuration of the antenna elements makes it difficult to be applied in a hand phone.

A good and practical diversity antenna for mobile terminals should have a low signal correlation between the antenna elements, an equal mean SNR for the receiving branches, and a relatively good matching characteristic of the input impedance [7]. In this paper, a novel dual-band printed diversity antenna for mobile terminals is proposed, and it fulfills all these criteria. The antenna with two back-to-back monopoles is printed on a PCB. Several ground branches are introduced to increase the isolation or adjust the resonant frequency. In Section II, the geometry of the proposed dual-band diversity antenna with some detailed dimensions is provided. And for the purpose of analyzing the antenna performance, a test-antenna geometry is defined. In Section III, the effects of some important parameters of the proposed antenna are fully discussed to show how this diversity antenna works. And a design methodology is given afterwards. Following the design rules of the proposed antenna, a prototype operating at UMTS and 2.4-GHz WLAN is constructed in Section IV. In this section, the scattering parameters and the far-field radiation patterns of the prototype are obtained by experiments. Based on these measured data, the envelope correlation coefficient, the mean effective gains (MEGs), and the diversity gain are also calculated. Results show that the proposed antenna is a good candidate for diversity system. Finally, a conclusion is given in Section V.
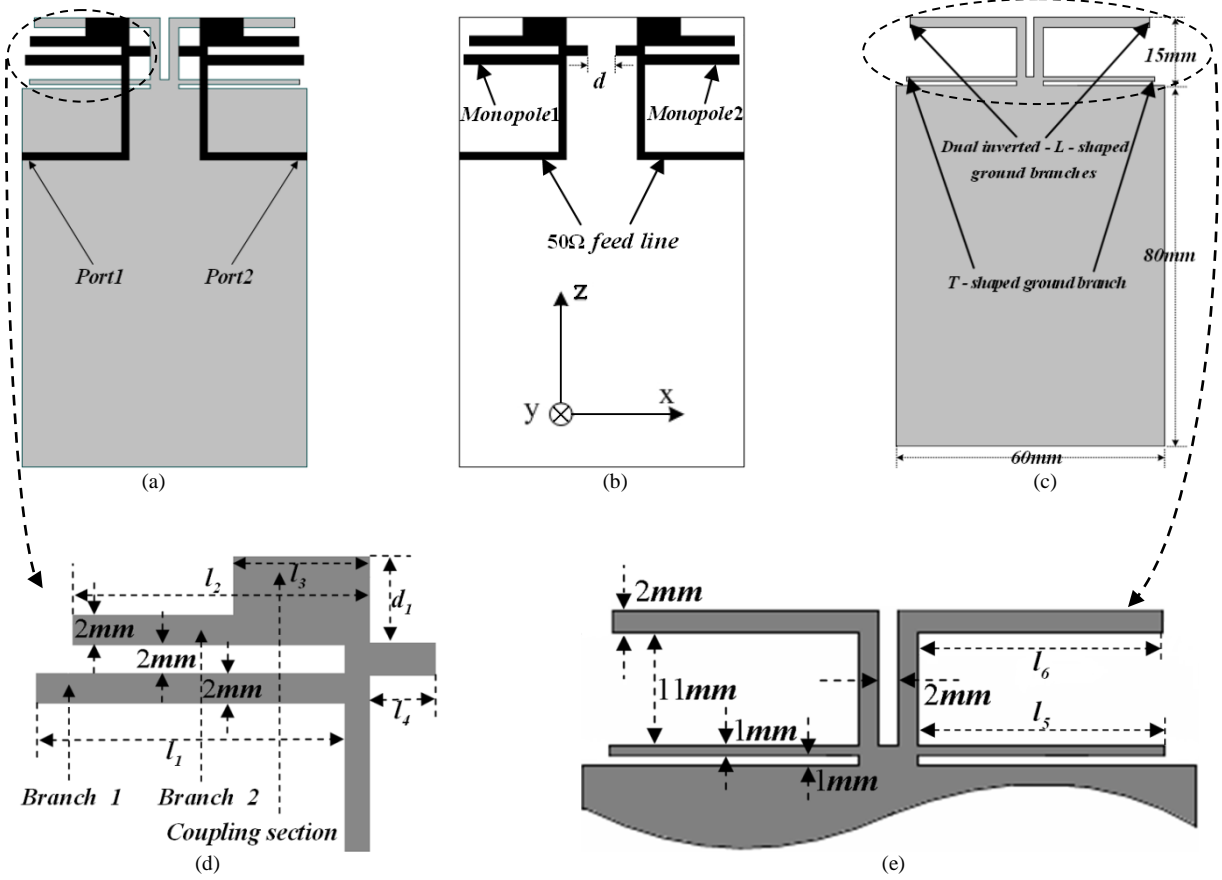
Fig. 1. Configuration of the proposed diversity antenna: (a) general view; (b) top view; (c) back view; (d) dimensions of the antenna structure; (e) dimensions of the ground branches.

II. ANTENNA CONFIGURATION

The specific geometry with some detailed dimensions of the proposed antenna is illustrated in Figure 1. The diversity antenna consists of two symmetric back-to-back multi-branch monopoles with a height of only 15 *mm*. It is printed on the upper part of a partially grounded FR4 substrate with dimensions $95 \times 60 \times 0.8$ *mm^3* and relative permittivity 4.4. On the back surface of the substrate, the main rectangular ground plane of 60 *mm* in width and 80 *mm* in length is printed and treated as the whole circuit part in a mobile terminal. In order to increase the isolation between two monopoles or adjust the resonant frequency, a T-shaped and dual inverted-L-shaped ground branches are introduced. Because the widths of the branches, both in monopole elements and ground structure, do not affect the antenna performance much, they are specified as 1 *mm* or 2 *mm* in this paper as shown in Figure 1.

To analyze the performance of the antenna, it is useful to define the initial dimensions of a test-antenna geometry. For the test geometry the dimensions of monopole branches are (l_1, l_2, l_3, l_4, d_1) = (20 *mm*, 18 *mm*, 9 *mm*, 4.5 *mm*, 6 *mm*). And the lengths of the ground branches are (l_5, l_6) = (25 *mm*, 24 *mm*). The antenna can be set up in a mobile handset, leaving enough space for the circuit part and reducing the effect of human hands. In Section IV, the test-antenna dimensions are modified to produce an antenna suitable for UMTS and 2.4-GHz WLAN applications.

III. THE ANALYSES BASED ON SIMULATED RESULTS

From the simulated results, we can know why the proposed antenna has two resonant frequencies, what affect them, and what structure can increase the isolation between two monopoles. Furthermore, some physical mechanism can be revealed, and a design methodology of this kind diversity antenna is obtained.

The performance of the proposed diversity antenna, especially the scattering parameters S_{11} and S_{21} (because of the symmetric configuration, S_{22} (S_{12}) is consistent with S_{11} (S_{21})), is analyzed by varying different parameters, while keeping the remaining dimensions of the antenna geometry fixed as for the test geometry defined in Section II.

In this paper, the simulated results are all obtained by High-Frequency Structure Simulator (HFSS) [9] software Version 9.2.

1) The effects of the antenna parameters on S_{11}

1a) The effects of the antenna parameters on the high resonant frequency

Among the parameters marked in Figure 1, only l_1 and l_2 can affect or dominate the high resonant frequency obviously.

In Figures 2 and 3 we present the S_{11} characteristics for several l_1 and l_2. It can be noticed that the increase of l_1 or l_2 reduces the high resonant frequency with generally better matching.
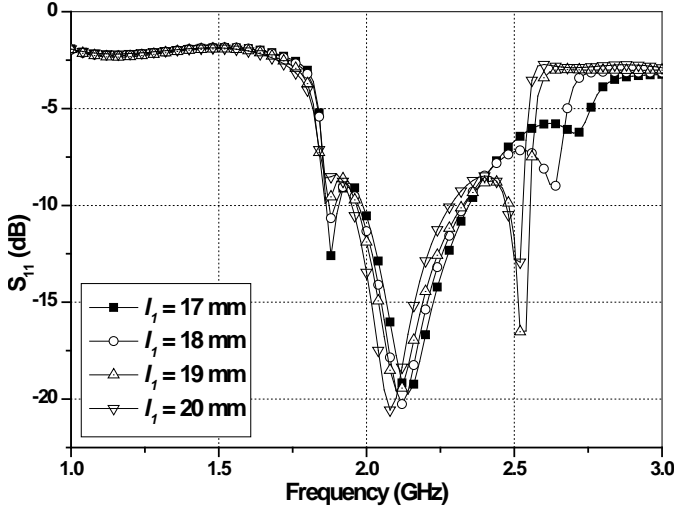
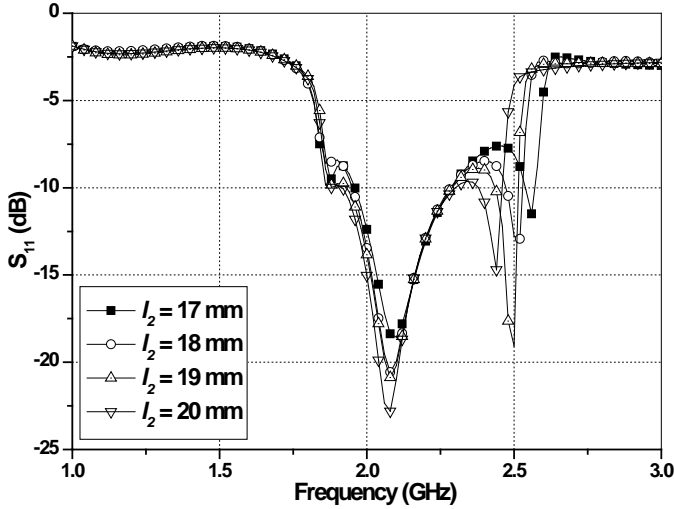Fig. 2. S_{11} against frequency with different l_1.

Fig. 3. S_{11} against frequency with different l_2.

At the beginning of the design, the branch 1 (with the length l_1) and branch 2 (with the length l_2) are expected to make the antenna exhibit dual-band characteristic because they present two surface current paths with different lengths. However, from Figure 3 the low resonant frequency does not change much while varying the parameter l_2, which determines the length of the longer surface current path. The reason will be analyzed in Section III *1) 1b)*.

1b) The effects of the antenna parameters on the low resonant frequency

In order to know which structure makes the antenna operate at the low resonant frequency, the radiation mechanism within this band should be revealed. For the test-antenna, when monopole 1 is excited at 2.12 GHz (2.12 GHz is the center frequency of the low band for the test-antenna), the vector current distributions both on monopole 1 and the ground structure are given in Figure 4. The current on the monopole 1 is mainly concentrated on the branch 2 and a protruding block above it (we call it the coupling section marked in Figure 1).

Because of the existence of the coupling section, strong current is evoked in phase on the corresponding (the left one in Figure 4 (b)) inverted-L-shaped ground branch. At the same time, the current with opposite phase on the other one (the right inverted-L-shaped ground branch in Figure 4 (b)) can be observed. As a consequence, the dual inverted-L-shaped ground branches can be regarded as a dipole due to the similar current distribution [10]. Thus, we can conclude that the radiation within the low resonant frequency band is contributed by branch 2 and the "dipole". In other words, the low resonant frequency of the antenna is determined by parameters l_2 and l_6 together.

In Figure 5 we can observe obviously that the center frequency of the low band is reduced by increasing l_2 and l_6 simultaneously. The result appeared at the high resonant frequency has been given in Section III *1) 1a)*.

2) The effects of the antenna parameters on S_{21}

For the test-antenna, two notches on the S_{21} curve, which represents the isolation between two monopoles, can be seen in Figure 6. According to the characteristic of the frequency, we call them the high notch and the low notch respectively, and the corresponding resonant frequencies are f_{nh} and f_{nl} marked in Figure 6.

2a) The effects of the antenna parameters on the high notch

Because the two monopoles with a common ground are placed very close, and the branches of them are parallel, relatively strong near field and ground current coupling must exist. For the test-antenna, the average current distributions both on monopole 2 and the ground structure are depicted in Figure 7 when monopole 1 is excited at 2.55 GHz (f_{nh}). It can be observed that there is still strong current on the monopole 2 and the ground beneath it. Thus we can believe that the near field coupling should be mostly offset by the ground current coupling at around f_{nh}. So the frequency of the high notch must be determined by the current both from the ground and the near field coupling. Because the main rectangular part of the ground plane is considered to be the system circuit board of a mobile terminal (chosen as 80×60 mm^2 in this paper), it cannot be changed arbitrarily, as well as the current on it. The current caused by near field coupling must be dominated by both the near field (evoked by the incentive element) and the coupling path. So the changes of radiation branches (branches 1 and 2), which contribute the near field and coupling path between two monopoles mostly, can affect the high notch frequency (f_{nh}) obviously. In Figures 8 and 9, the S_{21} parameters of the proposed antenna with different l_1 and l_2 are presented respectively. From the Figures, the same rules can be obtained: as the l_1 or l_2 increases, the f_{nh} decreases without changing the low notch.
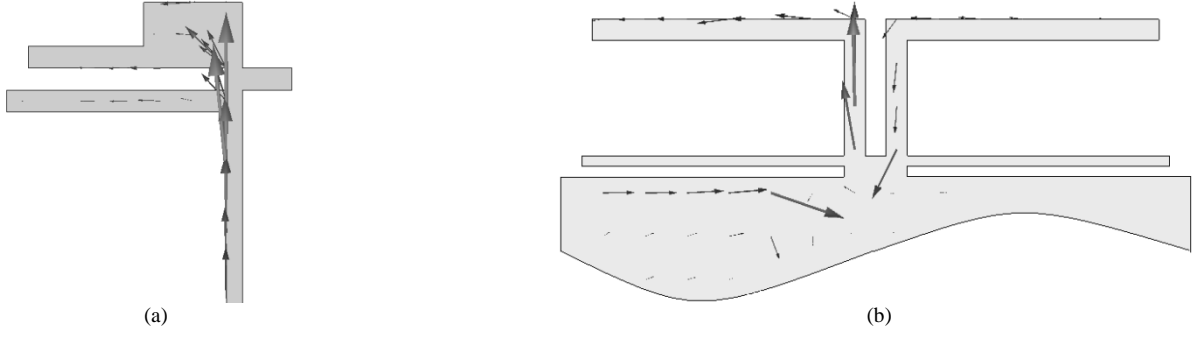
Fig. 4. The vector current distributions for the test-antenna with port1 excitation at 2.12 GHz: (a) the multi-branch monopole 1; (b) the ground structure.
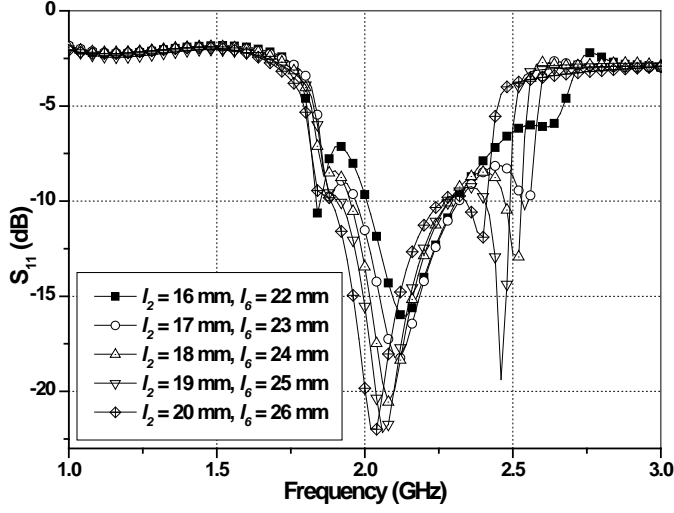

Fig. 5. S_{11} against frequency with different l_2 and l_6.
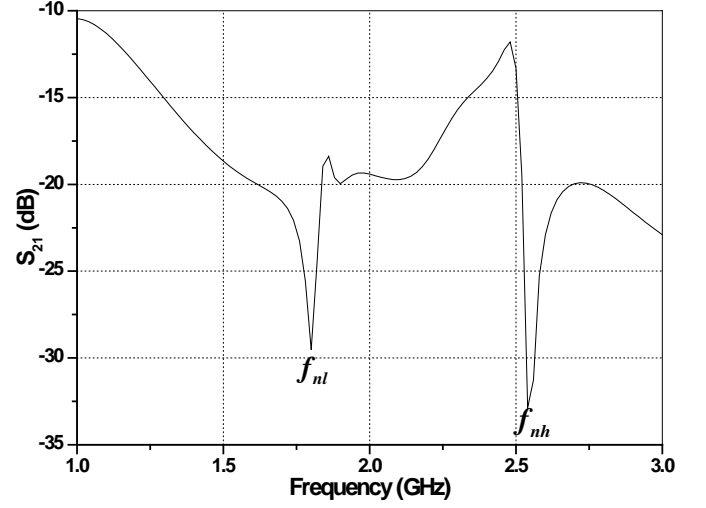

Fig. 6. S_{21} against frequency of the test-antenna.

Fig. 7. The average current distributions for the test-antenna with port1 excitation at 2.55 GHz (the light color means large current density): (a) the multi-branch monopole 2; (b) the ground structure.

2b) The effects of the antenna parameters on the low notch

Based on much research work, we have found out that there will be no low notch without the T-shaped ground branch. And if the parameters of the T-shaped ground branch are fixed, the low notch will be changeless. Figure 10 describes the distribution of the average current density on the ground structure with port1 excitation at 1.8 GHz (f_{nl}) for the test-antenna. It is noticed that strong current exists on both sides

of the corresponding slot (the left one) formed by the T-shaped ground branch. The x and z components of the $\vec{E}$ field in the substrate are presented in Figure 11. The length of the arrowhead is proportional to the $\vec{E}$ field strength. The one towards negative x-direction contributes to the energy coupling between the monopole 1 and the T-shaped ground branch. The strong $\vec{E}$ field across the slot means a strong radiation of energy. It seems that one arm of the T-shaped ground branch

could form a slot antenna with an open
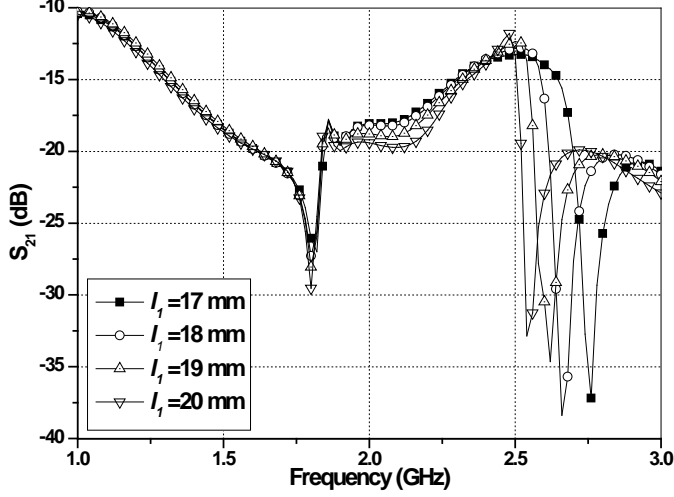
Fig. 8. S$_{21}$ against frequency with different l_1.

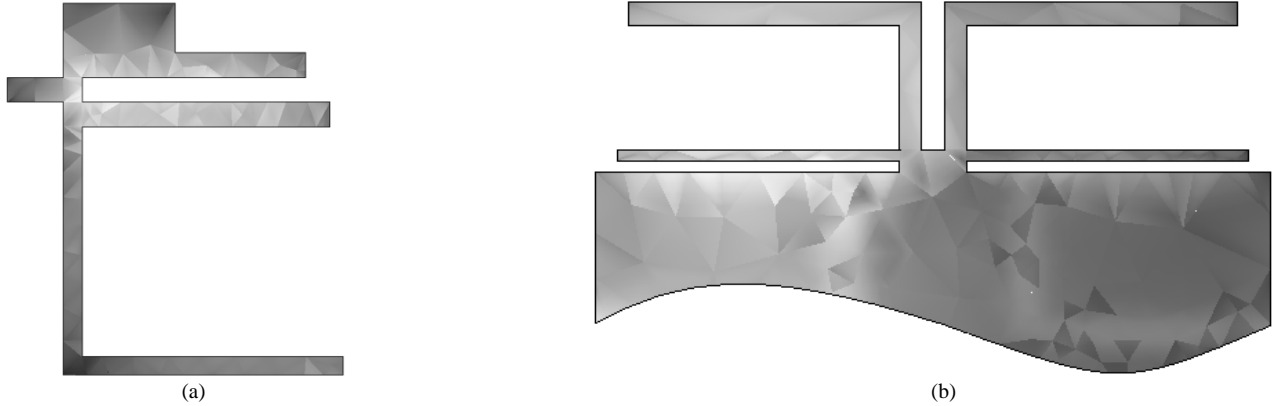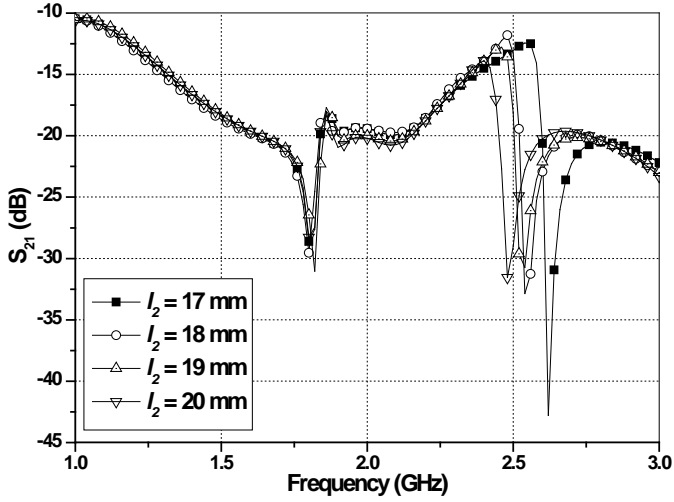Fig. 9. S$_{21}$ against frequency with different l_2.
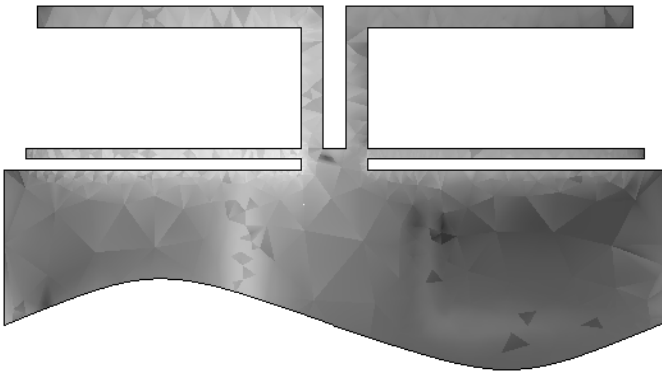
Fig. 10. The average current distribution on the ground plane for the test-antenna with port1 excitation at 1.8 GHz (the light color means large current density).

end, which has a resonant length of λ/4 [6]. If the effect of the substrate is considered, the "slot antenna" will operate at around 1.8 GHz for the test-antenna. This reasonable assumption tells us that when the "slot antenna" works, due to

the energy consumption by the radiation, there will be much
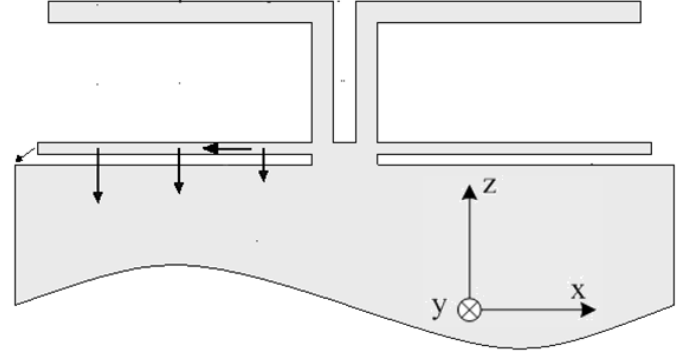
Fig. 11. The x and z components of the $\vec{E}$ field in the substrate for the test-antenna with port1 excitation at 1.8 GHz (The length of the arrowhead is proportional to the $\vec{E}$ field strength).
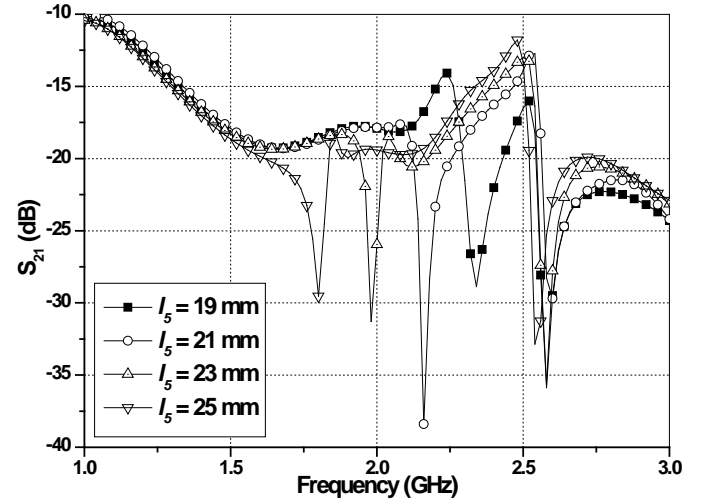
Fig. 12. S$_{21}$ against frequency with different l_5.
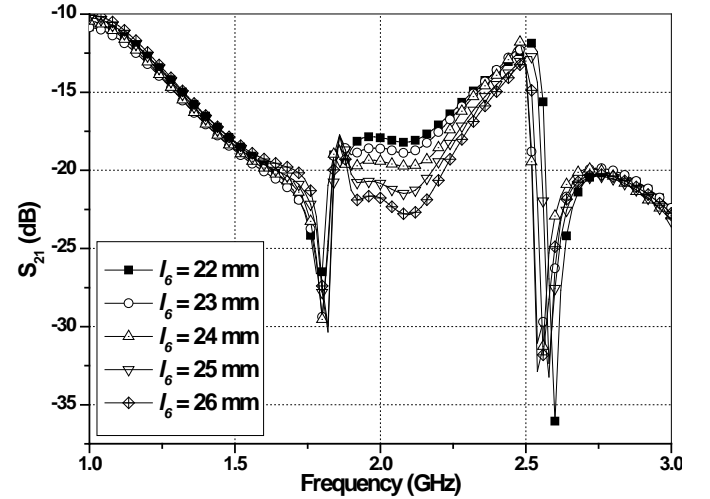
Fig. 13. S$_{21}$ against frequency with different l_6.

weaker coupling between two monopoles. As shown in Figure 12, the low notch on the S$_{21}$ curve reduces remarkably with the increase of the parameter l_5 (the length of the arms of the T-shaped ground branch).

3) Summary of the each parameter's effects on the antenna performance

In Sections III *1)* and *2)*, by exposing the physical mechanism of the proposed diversity antenna, each structure's function and the important parameters' effects are analyzed. In order to obtain a design methodology, each parameter's effects on the antenna performance are listed as follows.

- l_1 : adjusts the high resonant frequency and its matching characteristic; adjusts the frequency of the high notch on the S_{21} curve.
- l_2 : adjusts the high resonant frequency and its matching characteristic; adjusts the frequency of the high notch on the S_{21} curve; determines the low resonant frequency with the parameter l_6 together.
- l_3 : does not have much effect within a certain extent (only used for coupling energy to the corresponding inverted-L-shaped ground branch).
- l_4 , d_1 : adjusts the matching characteristic a little in both the high and the low resonant frequency bands.
- l_5 : adjusts the frequency of the low notch on the S_{21} curve.
- l_6 : adjusts the magnitude of the coupling within the band between the frequencies of the high and the low notches (as in Figure 13); determines the low resonant frequency with the parameter l_2 together.

4) The design methodology of the proposed dual-band diversity antenna

According to the rules concluded in Section III *3)*, it seems that we can design a dual-band diversity antenna with an excellent isolation between two monopoles. For instance, we can choose the values of the l_2 and l_6 to make the antenna operate at the desired frequency band, then adjust the parameter l_5 to move the low notch to that band. Unfortunately, in fact the case mentioned above doesn't work forever. If the low notch appears in that desired band, the monopole and the corresponding "slot antenna" are parallel connection relative to the feed line. As a consequence, the input resistance will be decreased almost by half in the band, and the matching characteristic will be deteriorated. Figure 14 illustrates the S_{11} parameters with different l_5 for the test-antenna, while the S_{21} parameters have been already shown in Figure 12. From Figure 14, it is found that the low resonant frequency is fixed to 2.12 GHz. When the value of the l_5 is 21 *mm*, the frequency of the low notch is between 2.1 and 2.2 GHz (as in Figure 12). And the input resistance at 2.12 GHz reduces to 20 Ω (it is 43 Ω when the value of l_5 is 25 *mm*). Thus, there will be a lot of energy reflection at port1.

According to all the analyses above, a design methodology for the dual-band diversity antenna is proposed as below.

- Determine the constraints on the main rectangular ground plane and the area occupied by the antenna according to the mobile terminal.
- Within the allowable area, adjust the l_2 and l_6 together to make the low resonant frequency meet the requirement. At the same time, it should be make sure that the energy transfer happens in the coupling section.
- Adjust the l_1 to change the high resonant frequency and the

high notch on the S_{21} curve.
- Alter the value of l_5 to make the low notch close to the low resonant frequency without destroying the matching characteristic.
- Tune, if necessary, l_4 and d_1 to obtain better matching characteristic within both bands.
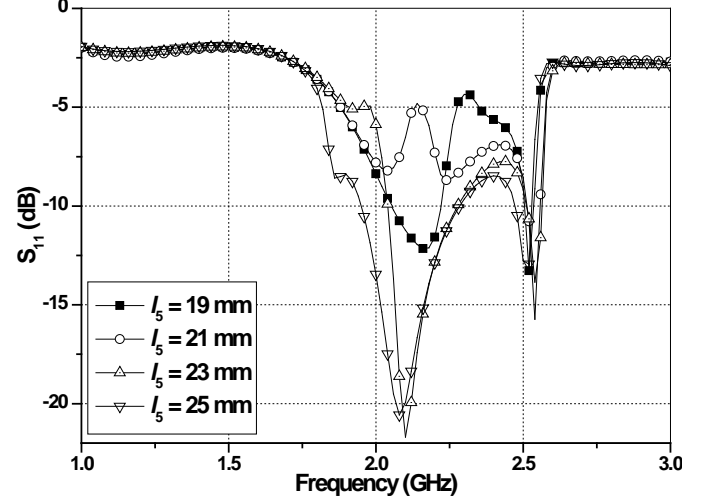
Fig. 14. S_{11} against frequency with different l_5.
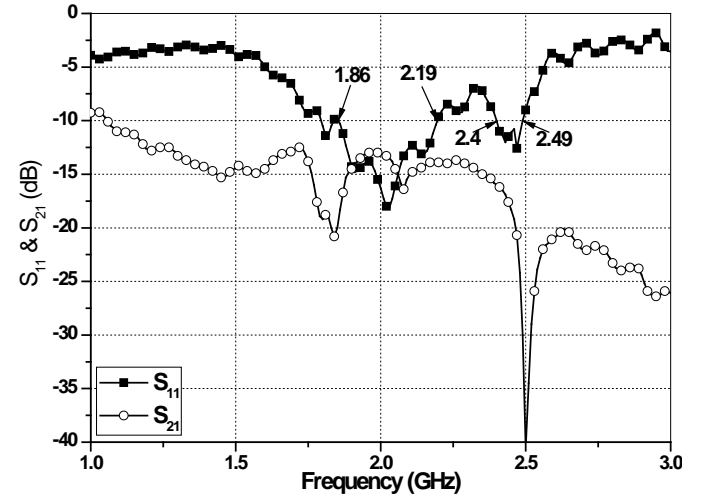
Fig. 15. Measured S_{11} and S_{21} against frequency for the prototype.

IV. A PROTOTYPE OF THE PROPOSED ANTENNA FOR UMTS AND 2.4-GHz WLAN APPLICATIONS

Using the methodology presented in the previous section, a dual-band diversity antenna for UMTS (1920 ~ 2170 MHz) and 2.4-GHz WLAN (2400 ~ 2484 MHz) operations is constructed and studied. The dimensions of the prototype are (l_1, l_2, l_3, l_4, d_1, l_5, l_6) = (21 *mm*, 21 *mm*, 9 *mm*, 4.5 *mm*, 6 *mm*, 27 *mm*, 27 *mm*). The prototype of the proposed antenna was measured and analyzed as follows.

1) Input characteristics

Under a selected combining scheme (that is to say, when the first element radiates, the other one is terminated to a 50-Ω
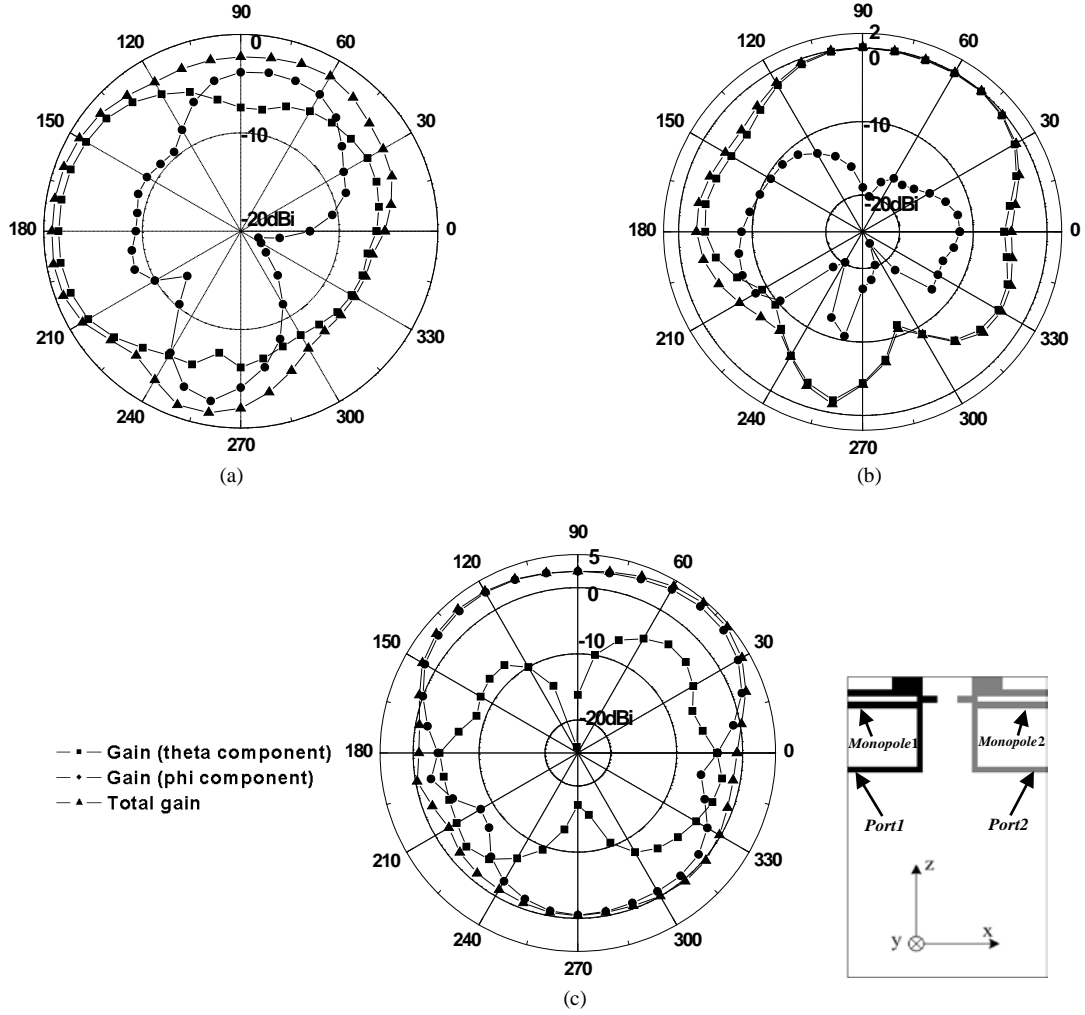
Fig. 16. Measured radiation patterns for monopole 1 at 2.05 GHz: (a) x-y plane; (b) x-z plane; (c) y-z plane.

impedance), the measured S_{11} and S_{21} of the prototype as a function of frequency are shown in Figure 15. The measured impedance bandwidths, defined by $S_{11} < -10$ dB, reach 330 MHz (1860 ~ 2190 MHz) and 90 MHz (2400 ~ 2490 MHz), which cover the required bandwidths of the UMTS and 2.4-GHz WLAN bands. Across the two bands, according to S_{21}, the isolations of the prototype, respectively, are larger than 13 dB and 16 dB.

2) Radiation patterns

Besides the scattering parameters, the active element patterns [11] (or coupled radiation patterns) of the diversity antenna are also studied. The active element patterns of an array are radiation patterns of the elements, which include all the mutual coupling effects between antenna elements, as well as the terminal loading effects. These patterns at 2.05 GHz were measured in an anechoic chamber. Figure 16 shows the patterns with monopole 1 excited and monopole 2 connected to a 50-Ω load. Figure 17 shows the patterns with the connections of monopoles 1 and 2 interchanged.

It should be noticed that, the maximum values of the gain patterns for monopoles 1 and 2 are almost identical but reflected in the axis of symmetry (y-axis). This may be due to

the presence of the dual inverted-L-shaped ground branches, which can also act as a reflector for each monopole. The measured active element patterns at 2.44 GHz which are not presented in this paper also show similar characteristics with those at 2.05 GHz. In general, the measured radiation patterns of these two monopoles cover complementary space regions. So the proposed antenna can provide pattern diversity in a wireless communication system.

3) The analysis methods of the correlation coefficient, the mean effective gains (MEGs) and the diversity gain

The correlation coefficient and relative signal-strength levels between received signals are required for determination of the diversity gain. The correlation coefficient of the received signals can be characterized by complex correlation coefficient ρ_{cij} ($i \neq j$) and the envelope correlation coefficient ρ_{eij}, which are related as below [12]:

$$\rho_{eij} \cong \left| \rho_{cij} \right|^2 \qquad (1)$$

where ρ_{cij} can be evaluated either from the mutual coupling (*mc*) between the antenna ports (ρ_{cij}^{mc}) or from the radiation
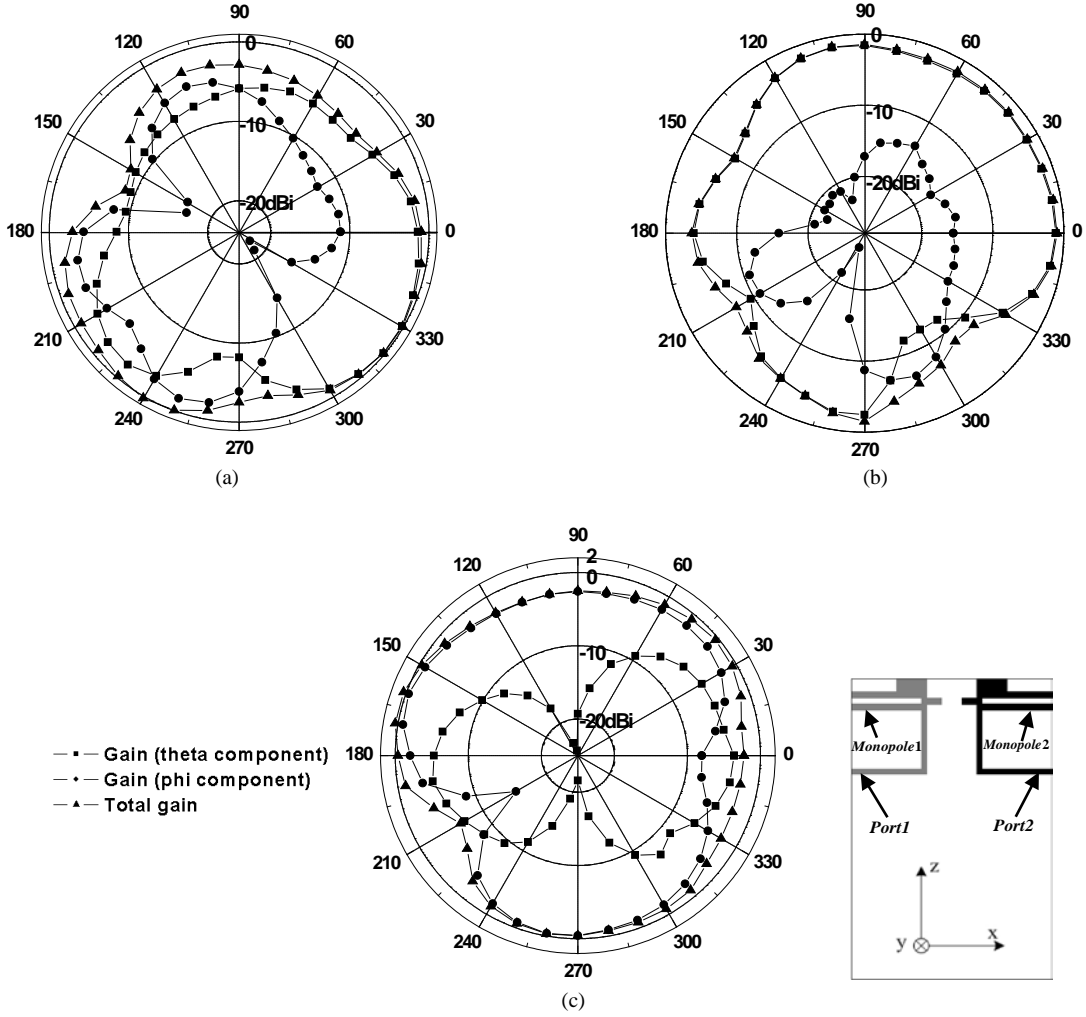
Fig. 17. Measured radiation patterns for monopole 2 at 2.05 GHz: (a) x-y plane; (b) x-z plane; (c) y-z plane.

patterns (*rp*) of the antenna elements and the statistics of the channel (ρ_{cij}^{rp}). The former one is obtained by the normalized mutual resistance $r_{ij} = Re(Z_{ij})/Re(Z_{ii})$ (where *Re* denotes the real part and Z_{mn} is the port impedance) using Eqn. (2) [1]

$$\rho_{cij}^{mc} \cong r_{ij} \qquad (2)$$

On the other hand, by using the radiation patterns and the statistics of the channel, the complex correlation can be calculated from Eqn. (3) [13]

$$\rho_{cij}^{rp} \cong \frac{\iint A_{ij}(\Omega)d\Omega}{\sqrt{\iint A_{ii}(\Omega)d\Omega \cdot \iint A_{jj}(\Omega)d\Omega}} \qquad (3)$$

where

$$A_{ij}(\Omega) = \Gamma \cdot E_{\theta i}(\Omega) \cdot E_{\theta j}^*(\Omega) \cdot p_\theta(\Omega) + E_{\varphi i}(\Omega) \cdot E_{\varphi j}^*(\Omega) \cdot p_\varphi(\Omega)$$

in which E_θ and E_φ are the θ and φ components of the complex electric field radiation pattern respectively and p_θ and p_φ are the θ and φ components of the probability distribution function of the incoming wave respectively. The asterisk denotes the complex conjugate. The parameter Γ is the cross-polarization discrimination (XPD) (ratio of vertical to horizontal power density) of the incident field. In this paper, Γ of 0 dB and 6 dB, which are the average in an indoor and an urban fading environment respectively [1], are assumed.

In general the results in (2) and (3) are not based on exactly the same assumptions but they should provide consistent estimates of ρ_{cij} [14]. So in this paper, we use the method of mutual coupling (a relatively fast method) to evaluate the correlation coefficient.

The mean power received from each antenna element can also be obtained from the radiation patterns and the statistics of the channel using the concept of the mean effective gain (MEG). The MEG of an antenna is defined as the ratio of the mean received power to the mean incident power of the antenna, given by [15]:

$$MEG = \iint \left[\frac{\Gamma}{1+\Gamma} \cdot p_\theta(\Omega) \cdot G_\theta(\Omega) + \frac{1}{1+\Gamma} \cdot p_\varphi(\Omega) \cdot G_\varphi(\Omega) \right] \cdot d\Omega \qquad (4)$$

where G_θ and G_φ are, respectively, the θ and φ polarized components of the antenna power gain pattern. The other

Frequency (GHz)	Isolation (dB)	Antenna efficiency (%)	ρ_{e12}^{mc}	MEG$_1$ (Γ=0dB) (dBi)	MEG$_2$ (Γ=0dB) (dBi)	MEG$_1$ (Γ=6dB) (dBi)	MEG$_2$ (Γ=6dB) (dBi)	Diversity gain (1%) (dB)	Bandwidth (S$_{11}$<−10dB) (GHz)
2.05	14.5	94.9	0.0144	−5.66	−5.13	−4.96	−4.36	9.935	1.86 ~ 2.19
2.44	17.6	90.3	0.0895	−9.52	−8.97	−8.68	−7.90	9.7523	2.40 ~ 2.49

Table 1. Performance of the prototype of the proposed diversity antenna

parameters have the same meanings as defined in (3). The angular density functions and the gains are normalized as [16]

$$\iint p_\theta(\Omega)d\Omega = \iint p_\varphi(\Omega)d\Omega = 1 \qquad (5)$$

$$\iint \left[G_\theta(\Omega) + G_\varphi(\Omega) \right] d\Omega = 4\pi \cdot \eta \qquad (6)$$

where η represents the radiation efficiency of the antenna. The mobile wireless environment defined in [14] has a series of reasonable assumptions: the fading envelope being Rayleigh distributed, the incoming field arriving in horizontal plane only, the incoming field's orthogonal polarizations being uncorrelated, the individual polarizations being spatially uncorrelated, and finally the time-averaged power density per steradian being constant. Based on these approximations, the MEG can be written as

$$MEG = \frac{1}{2\pi} \cdot \int_0^{2\pi} \left[\frac{\Gamma}{1+\Gamma} \cdot G_\theta(\frac{\pi}{2},\varphi) + \frac{1}{1+\Gamma} \cdot G_\varphi(\frac{\pi}{2},\varphi) \right] \cdot d\varphi \qquad (7)$$

In an antenna diversity system, diversity gain, which is the amount of improvement obtained from a multiple element antenna system relative to a single element one, is one of the most important parameters. In this paper, the diversity gain of the prototype under selected combining scheme is calculated based on the correlation coefficient and the MEGs [17] which are obtained from the measured data.

4) Summary of the performance of the prototype

The performance of the prototype of the proposed dual-band printed diversity antenna including the envelope correlation coefficient, the MEGs and the diversity gain at 1% of the cumulative distribution functions (CDFs) is listed in Table 1.

From the table, it is found out that the diversity antenna meets the demand of UMTS/WLAN (2.4-GHz) dual-band operations with high antenna efficiency and good isolation between the two monopoles. Furthermore, the received signals satisfy the conditions $\rho_{e12} < 0.5$ and $P_1 \approx P_2$ (|MEG$_1$/MEG$_2$| <3 dB) [1]. As a consequence, the high diversity gains in both bands are obtained.

V. CONCLUSION

A novel dual-band printed diversity antenna for mobile terminals has been investigated in this paper. Based on many simulated results, a design methodology of this dual-band diversity antenna is provided. A prototype is constructed using this design methodology. The measured -10 dB bandwidths are 1.86 to 2.19 GHz and 2.40 to 2.49 GHz with acceptable isolation over the bandwidths. The envelope correlation coefficient and the MEGs of the antenna elements are calculated from the measured radiation patterns. We have shown that the envelope correlation coefficients of the diversity antenna are less than 0.5, the MEG ratios are maintained close to unity and the diversity gains almost reach 10 dB in both bands. It is proved that the proposed antenna can achieve high performance for diversity and is very suitable for mobile terminals.

REFERENCES

[1] R. G. Vaughan and J. B. Andersen, "Antenna diversity in mobile communications," *IEEE Trans. Veh. Technol.*, Vol. VT-36, pp. 149-172, Nov. 1987.
[2] D. Gesbert, M. Sha, D. S. Shiu, P. Smith, and A. Naguib, "From theory to practice: An overview of MIMO space-time coded wireless systems," *IEEE J. Select. Areas Commun.-Spec. Issue MIMO Syst.*, Vol. 21, pp. 281-302, Apr. 2003.
[3] Tzuenn-Yih Wu, Shyh-Tirng Fang, and Kin-Lu Wong, "Printed diversity monopole antenna for WLAN operation," *Electronics Letters*, Vol. 38, No. 25, pp. 1625-1626, 5th Dec. 2002.
[4] Kin-Lu Wong, An-Chia Chen, and Fa-Shian Chang, "Planar diversity-loop antenna for wireless PCMCIA card," *Microwave and Optical Technology Letters*, Vol.39, No. 6, 20th Dec. 2003.
[5] Gaoming Chi, Binhong Li, and Dongsheng Qi, "Dual-band printed diversity antenna for 2.4/5.2-GHz WLAN application," *Microwave and Optical Technology Letters*, Vol. 45, No. 6, pp. 561-563, 20th Jun. 2005.
[6] Saeed I. Latif, Lotfollah Shafai, and Satish Kumar Sharma, "Bandwidth enhancement and size reduction of microstrip slot antennas," *IEEE Trans. Antennas Propag.*, Vol. 53, No. 3, pp. 994-1003, Mar. 2005.
[7] H. T. Hui, "Practical dual-helical antenna array for diversity/MIMO receiving antennas on mobile handsets," *IEE Proc.-Microw. Antennas Propag.*, Vol. 152, No. 5, pp. 367-372, Oct. 2005.
[8] C. C. Chiau, X. Chen, and C. G. Parini, "A compact four-element diversity-antenna array for PDA terminals in a MIMO system," *Microwave and Optical Technology Letters*, Vol. 44, No. 5, pp. 408-412, Mar. 2005.
[9] Ansoft Corporation HFSS, http://www.ansoft.com/products/hf/hfss.
[10] Huey-Ru Chuang, and Liang-Chen Kuo, "3-D FDTD design analysis of a 2.4-GHz polarization-diversity printed dipole antenna with integrated balun and polarization-switching circuit for WLAN and wireless communication applications," *IEEE Trans. Microwave Theory Tech.*, Vol. 51, No. 2, pp. 374-381, Feb. 2003.
[11] David F. Kelly, and Warren L. Stutzman, "Array antenna pattern modeling methods that include mutual coupling effects," *IEEE Trans. Antennas Propag.*, Vol. 41, No. 12, pp. 1625-1632, Dec. 1993.
[12] R. H. Clarke, "A statistical theory of mobile radio reception," *Bell Syst. Tech. J.*, pp. 957-1000, 1968.
[13] K. Boyle, "Radiation patterns and correlation of closely spaced linear antennas," *IEEE Trans. Antennas Propagat.*, Vol. 50, No. 8, Aug. 2002.
[14] Samuel C. K. Ko, and Ross D. Murch, "Compact integrated diversity antenna for wireless communications," *IEEE Trans. Antennas Propagat.*, Vol. 49, No. 6, pp. 954-960, Jun. 2001.
[15] T. Taga, "Analysis for mean effective gain for mobile in land mobile radio environments," *IEEE Trans. Veh. Technol.*, Vol. 39, No. 2, pp. 117-131, May 1990.
[16] G. F. Pedersen and J. B. Andersen, "Handset antennas for mobile communications: Integration, diversity and performance," *Rev. Radio Sci. 1996-1999*, pp. 119-133, Aug. 1999.
[17] W. C. Lee, "Mobile Communications Engineering," 2nd ed. New York: McGraw-Hill, 1998, pp. 351-357.

Yuan Ding was born in Xinjiang Autonomous Region, China, on November 12, 1981. He received the Bachelor's degree from Beihang University (BUAA), Beijing, China, in 2004. Now he is pursuing the Master's degree with Department of Electronic Engineering, Tsinghua University, Beijing, China.

His research interests are in multi-antenna design and wireless channel modeling.

Zhengwei Du was born in Sichuan Province, China, on August 21, 1971. He received the Bachelor's, Master's, and Doctoral degrees in engineering from the University of Electronic Science and Technology of China, Chengdu, China, in 1992, 1995, and 1998, respectively.

Since 1998, he has been with Tsinghua University, Beijing, China, as a Postdoctoral Fellow (February 1998-October 1999), Research Assistant (November 1999-July 2000), Associate Professor (August 2000-December 2006), and, currently, Full Professor. His main research interests include ultra wideband/short pulse electromagnetic, antenna, propagation, analysis of microwave/millimeter wave planar structures, photonic bandgap (electromagnetic bandgap) circuits, and electromagnetic compatibility / electromagnetic interference (EMC/EMI).

Prof. Du is Chairman of the Microwave Integrated Circuits and Mobile Communications Professional Committee of the Microwave Society of China.

Ke Gong received the Bachelor's and Doctoral Degrees in technical science from Beijing Institute of Technology (BIT), Beijing, China, in 1982 and Technical University of Graz, Austria, in November 1986, respectively.

From 1987-2006, he worked in Tsinghua University on wireless channel characteristics, broadband wireless access, antenna, and terrestrial Digital TV transmission, etc.

Prof. Gong is now with Tianjin University and vice chairman of China Institute of Communications (CIC), vice chairman of Chinese Institution of Electronics (CIE).He is member of IEEE AP, Comsoc and MIT, too.

Zhenghe Feng (A'01) graduated from the Department of Radio and Electronics, Tsinghua University, Beijing, P. R. China, in 1970.

Since 1970, he has been with Tsinghua University as an Assistant, Lecturer, Associate Professor, and Full Professor. His main research areas include numerical techniques and computational electromagnetics, radio frequency and microwave circuits and antennas, radio frequency and microwave digital communication systems, smart antennas, and spatial-temporal signal processing.

Prof. Feng is the Vice Chair of the Microwave Society, Chinese Institute of Electronics (CIE), and Deputy Chairman of IEEE Microwave Theory and Techniques (MTTs) Beijing Chapter.